Integrated air quality modeling for urban policy: A novel approach with olympus-chimere

Arthur Elessa Etuman, Isabelle Coll

Atmospheric Environment 315 (2023) 120134

Contents lists available at ScienceDirect

Atmospheric Environment

journal homepage: www.elsevier.com/locate/atmosenv

Integrated air quality modeling for urban policy: A novel approach with olympus-chimere

Arthur Elessa Etuman [a,b,*], Isabelle Coll [a]

[a] Laboratoire Interuniversitaire des Systèmes Atmosphériques (LISA), UMR CNRS 7583, Université Paris Est Créteil et Université Paris Cité, Institut Pierre Simon Laplace (IPSL), Créteil, France
[b] SPLOTT, Systèmes Productifs, Logistique, Organisation des Transports, et Travail, Univ Gustave Eiffel, AME-SPLOTT, F-77454 Marne-la-Vallée, France

HIGHLIGHTS

- Description of an air quality modeling chain for decision-making.
- Integration of socio-demographics parameters in the air pollutant emissions and concentrations modeling.
- Validation of the modeling chain on Paris megacity.

GRAPHICAL ABSTRACT

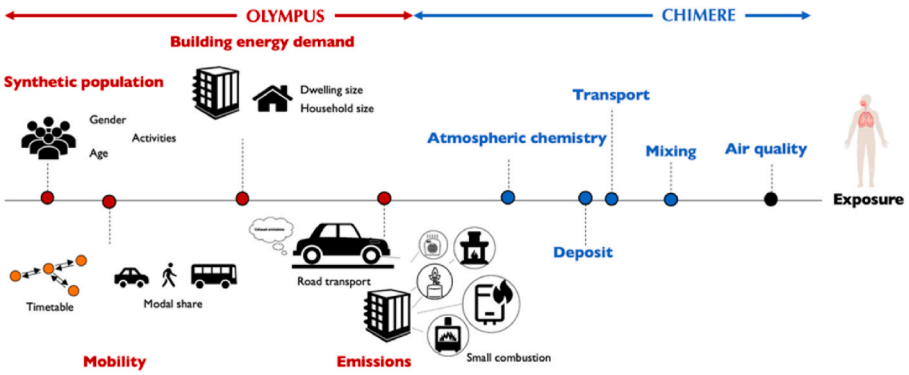

ARTICLE INFO

Keywords:
Air pollution
Air quality modeling
Emissions
Urban policies
Road transport

ABSTRACT

This paper presents a novel approach to air quality modeling for megacities, focusing on the Paris region for the year 2009. The simulation is conducted by coupling the transport, energy demand, and emission model OLYMPUS with the atmospheric chemical transport model CHIMERE. OLYMPUS's emission calculations are based on the representation of an urban configuration, the simulation of a synthetic population, and the calculation of transport demand and energy consumption in buildings using an activity-based statistical approach. Emissions derived from this simulation, along with biogenic and additional industrial emissions, were used as input data in the CHIMERE model to predict pollutant concentrations. CHIMERE outputs were compared with observations from the local AIRPARIF air quality monitoring network, and with a reference simulation conducted using a benchmark bottom-up emission inventory. The results indicate that the platform provides a comprehensive representation of emissions and the resulting air quality. They also highlight the excellent representation of the spatial and temporal distribution of urban pollutant concentrations in comparison with both model and observational data. OLYMPUS tends to emit more primary pollutants than the reference emission inventory in the dense urban center. However, this often improves model scores for NO_2, and these deviations remain within the uncertainty margins set for emission inventories. The approach to emission production, rooted

* Corresponding author. Laboratoire Interuniversitaire des Systèmes Atmosphériques (LISA), UMR CNRS 7583, Université Paris Est Créteil et Université Paris cité, Institut Pierre Simon Laplace (IPSL), Créteil, France.
E-mail address: arthur.elessa-etuman@lisa.ipsl.fr (A. Elessa Etuman).

https://doi.org/10.1016/j.atmosenv.2023.120134
Received 6 June 2023; Received in revised form 27 September 2023; Accepted 7 October 2023
Available online 13 October 2023

in the connection between urban configuration and individual behaviors, allows for the exploration of innovative air quality scenarios centered on energy consumption practices. The validation of our results furnishes the OLYMPUS-CHIMERE coupling with a dependable framework for addressing numerous research inquiries related to the impact of urban policies on air quality.

List of acronyms

Airparif	Ile-de-France air quality monitoring network
ARENE	Regional Agency for the Environment and New Energies
ARPEGE	Global numerical weather prediction model (Météo France)
CEREN	French Center for Economic studies and Research on ENergy
CHIMERE	Eulerian Chemical Transport Model
CITEPA	Interprofessional technical center for the study of atmospheric pollution
COPERT	Computer Program to Calculate Emissions from Road Transport
CTM	Chemical Transport Model
ECMWF	European Centre for Medium-Range Weather Forecasts
EEA	European Environment Agency
EGT	Global Transport Survey
EMEP	European Monitoring and Evaluation Programme
EURO	European emissions standard for vehicles
GTFS	General Transit Feed Specification (Data format for public transport schedules)
HTAP	Emission database from the Hemispheric Transport of Air Pollution initiative
INSEE	French National Institute for Statistics and Economic Studies
IRIS	Grouped islands for statistical information
MEGAN	Model of Emissions of Gases and Aerosols from Nature
PM	Particulate Matter
SNAP	Standard Nomenclature for Air Pollution
STIF	Île-de-France public transport authority
TNO	Independent research body in the Netherlands.
UDI	Urban Density Index
WRF	Weather Research and Forecasting (Numerical prediction tool)

1. Introduction

Whether indoors or out, the air we breathe is contaminated by fine atmospheric particles and a plethora of gaseous pollutants, posing significant health risks. These pollutants originate from both natural sources - including biogenic, dust, and volcanic emissions - and anthropogenic activities like industrial processes, road transport, agriculture, or commercial and domestic activities. Profound between air pollution and numerous respiratory and cardiovascular diseases, such as asthma, rhinitis, bronchitis, lung cancer, myocardial infarction, and stroke is now widely recognized (World Health Organization, 2013). In 2012, the World Health Organization (WHO) reported that ambient air pollution was responsible for 3.7 million deaths worldwide (World Health Organization, 2016). The populations affected are overwhelmingly urban, living in metropolises whose attractiveness, size and density are increasing, and where the question of emissions and exposure to air pollution has become a major public health issue (European Environment Agency). Furthermore, numerous studies indicate that exposure is unequally distributed among population groups, disproportionately impacting children, the elderly, those living near major roads, and individuals with limited healthcare access or pre-existing health conditions (Fairburn et al., 2019; Pascal et al., 2013). Therefore, pollution must be viewed as an urban issue, with a focus on mobility, transportation, and individuals.

Air pollution is one of the main challenges facing urban areas. In Europe, regulatory thresholds for particulate matter (PM) and nitrogen dioxide are regularly exceeded at traffic stations (European Environment Agency, 2018). Energy consumption and the combustion of fossil fuels significantly exacerbate urban pollution. In France, road transport constitutes one of the primary sources of nitrogen oxide and fine particle emissions in urban areas (CITEPA, 2014). Its pervasive presence in urban settings significantly influences the concentration patterns of atmospheric pollutants and the exposure of its residents. Cities, teeming with people and bustling with activity, are influenced by various determinants like planning, architecture, transport, energy, and environmental factors. Consequently, they are the primary source of urban pollution and have the greatest potential for implementing corrective measures. In light of this, urban organization has emerged as a critical issue. For instance, urban sprawl, identified as a significant problem in Europe, not only escalates environmental challenges by augmenting land and natural resource consumption but also encourages the expansion of peripheral residential and commercial regions, amplifying transportation demands to city centers and favoring private vehicle use. Conversely, while urban densification might mitigate sprawl and mobility needs, it could locally amplify pollutant emissions and heighten exposure for a larger segment of city inhabitants, intensifying public health worries. An integrated approach to exposure, which considers the interplay between urban planning, individual habits, transport, and socio-economic housing and population challenges, is crucial for addressing urban pollution. This perspective should allow us to better understand the emissions associated with various urban structures and evaluate the influence of urban policies on air quality.

To enhance urban air quality, contemporary environmental strategies have predominantly centered on minimizing emissions through advancements in combustion technologies. These involve guidelines like the European emission standards for vehicle exhaust gases (EURO) and refined pollutant capture methods in large combustion plants. Nonetheless, at the local level, dedicated urban planning, changes in mobility behaviors as well as the promotion of soft modes and non-fossil fuel energy sources for the realization of daily activities have been identified as efficient strategies to complement the technological efforts and help reduce air pollutant emissions. However, these levers are not easy to mobilize. Their impact can be undermined by a lack of opportunity for changing practices or by rebound effects in mobility. This is why, in addition to usual atmospheric processes, environmental research must consider the processes that govern cities - including mobility, energy consumption and transportation logistics - to produce a better assessment of the expected impact of urban policies on air quality and exposure.

Numerical air quality modeling, when capturing both key urban and atmospheric processes, can serve as a reliable guide for evaluating urban planning decisions. Recent literature highlights examples of new modeling platforms that integrate parameters such as transportation networks, employment centers, activities, traffic demand, emission factors and street geometry into air quality modeling. The stated aim is

to capture the impact of urban planning on air quality, and to offer a more holistic approach to modeling the urban environment. Examples include Hülsmann et al. (2014) with the MATSIM-OSPM platform in Munich, and Hatzopoulou and Miller (2010) with the TASHA-EMME-Mobile6-CALPUFF chain for Toronto. However, these platforms do not consider the so-called "small" (in reference to the boiler capacities) component of combustion emissions that arises from the residential, institutional and commercial sectors. In cities like Paris, these emissions constitute a significant proportion of total urban emissions - 20% of nitrogen oxides, 30% of volatile organic compounds, 30% of PM_{10} and 39% of $PM_{2.5}$ emissions (Airparif, 2013) - and therefore represent an important lever for reducing emissions. This sector, as in many other European countries, is one of the main levers for reducing pollutant emissions (European Environment Agency, 2018). Research must develop new modeling platforms that take into account air quality levers and are capable of modeling the impact on pollutant emissions of changes in energy consumption practices or in city organization, in the most holistic and activity-based approach possible. This should make it possible to identify new solutions for tackling air quality and environmental health in cities.

This work presents the implementation and evaluation of an air quality simulation over a French region, using an innovative modeling platform that integrates the various aspects of urban functioning into its environmental diagnosis. The platform relies on two main models. The OLYMPUS tool which constitutes the innovative element of this platform, has been developed to script air quality scenarios based on urban planning, transport use and energy consumption hypotheses. It displays the target urban situation and calculates the associated emissions of atmospheric pollutants, based on the activities of city dwellers. These activities include the various motives for daily mobility as well as energy consumption in the buildings, primarily for heating and hot water provision. Thus, OLYMPUS offers the advantage of taking into account in a single simulation the emissions linked to journeys in the city and those from small combustion appliances in domestic and commercial buildings. The second model of the platform is CHIMERE, a Eulerian Chemical Transport Model that simulates air pollutant concentrations as well as their spatial and temporal variability on a given domain, based on a state-of-the-art representation of atmospheric physical and chemical processes. In our platform, CHIMERE simulates air quality in the region of interest using the emissions inventory previously compiled by OLYMPUS. *In fine*, the mobility data produced by OLYMPUS are combined with air quality values from CHIMERE to produce a dynamic representation of the exposure of city dwellers in urbanized areas (Elessa Etuman et al., 2020).

The outline of this article is as follows. We will first present the operating principles (Section 2) and the implementation (Section 3) of the OLYMPUS-CHIMERE platform over the Greater Paris area. The outputs of the modeling platform will then (Section 4) be discussed and compared with outputs from a CHIMERE simulation using a state-of-the-art bottom-up emission inventory built from reporting data. The validation of the simulation should confirm the ability of the OLYMPUS CHIMERE platform to produce a relevant and comprehensive representation of air quality in a given urban situation, using an activity-based approach for emission calculation. Considering OLYMPUS's ambition to produce innovative urban scenarios for the assessment of population exposure, this work is an important step towards an advanced evaluation of public action for air quality and the improvement of associated public health outcomes.

2. The modeling chain description

The OLYMPUS-CHIMERE modeling chain has been set up to investigate the impacts of urban configuration, population practices and environmental policies on air pollutant emissions, air quality and exposure. It consists of 2 blocks which structures are presented in Fig. 1. The operating principles of these two blocks are detailed below.

2.1. OLYMPUS

The OLYMPUS emission model begins the modeling process by outlining a past, prospective, or hypothetical urban scenario. OLYMPUS considers key parameters of the targeted urban configuration to develop an emission inventory based on human activity. The model has four main components (refer to Fig. 1).

(1) a population generation module based on a conditional probabilities approach
(2) a mobility module based on attractiveness and practices of individuals
(3) a building energy demand module
(4) an air pollutant and Greenhouse Gases emission module

The modeling steps as well as the main operating processes of the OLYMPUS model can be summarized as follows. The first step in the modeling process is the categorization of the different areas of the territory. Urban zones are generally the result of a sub-municipal division. The categorization of different zones is essentially based on population density. Population density is an input to the model. In most simulations it can be derived from regional survey data. From these data, hypotheses are formulated to estimate the distribution of housing types (notably individual or collective buildings) in each spatial unit. This step determines household characterization and building density and defines the energy mix in the buildings. It also plays a role in the location of job centers and in the accessibility of spatial units. Finally, a synthetic

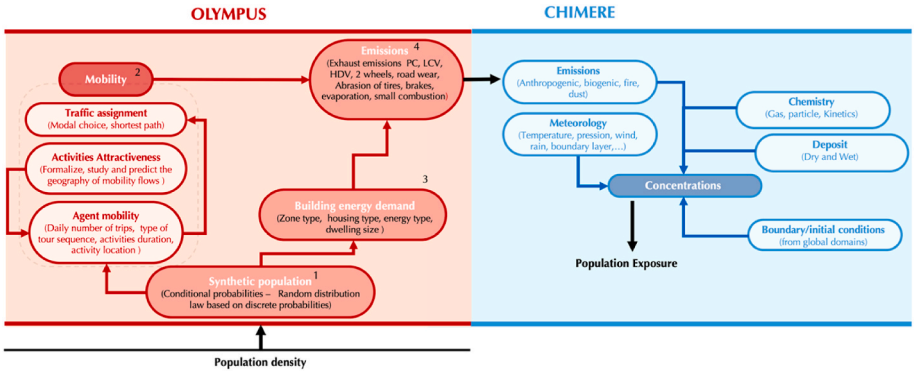

Fig. 1. Organization chart illustrating the OLYMPUS-CHIMERE modeling platform, as well as its main modules – The OLYMPUS model is composed of 4 main modules that generate (1) a synthetic population, (2) the mobility of each created population agent, (3) the energy demand of households and employment in the commercial sector and emissions associated with agent mobility and building energy demand. The CHIMERE model integrates these emissions and associates them with other emissions as well as physical and chemical data from the atmosphere to characterize pollutant concentrations.

population (modeled agents with socio-demographic attributes) is generated based on the INSEE survey data, following a conditional probability approach. The agent characteristics include for instance age, gender and socio-professional status, and are used to prefigure their daily activity loops in the city.

To define agent mobility, three mains modeling steps are required. The first one is the definition of the attraction potential of each of the zones identified in the administrative division. The attraction potential - also called attractiveness - can be defined as the probability of performing an activity in a given area. Attractiveness depends mainly on the density of activity considered (employment, school, leisure, shopping …) in the area.

Once the attractiveness of the activities has been defined, the model generates the mobility of each agent from the synthetic population. Mobility is constrained by priorities that are statistically assigned to each agent. The location where activities are carried out is based on both the attractiveness of the zones and the travel distance. The transport mode to get from one activity to another is selected by using a Multi-Nomial Logit (MNL) (McFadden, 1973) driven by a utility function. Finally, for each car trip, the model assigns the route to a transport network by calculating the shortest path using graph theory.

In parallel, OLYMPUS generates the energy demand of buildings in the residential, institutional, and commercial sectors. The calculation is based on parameters statistically attributed to households, such as the type and average surface area of each dwelling, as well as on unit consumption data per domestic agent. For the institutional and commercial sectors, modeling is based on unit consumption data per employee.

At last, emissions from the simulated activities are calculated using methodologies acknowledged by the European Environment Agency (EEA). For road transport, emission factors are taken from the software COPERT (Computer Program to Calculate Emissions from Road Transport) and include cold-start engine emissions as well as resuspension on the road. For small combustion in the residential, institutional and commercial sectors, the model applies a breakdown of energy sources based on survey data and using the Urban Density Index (UDI) and the type of housing as proxies.

OLYMPUS has demonstrated its ability to reproduce population specificities by learning from survey data, and to reproduce population mobility practices such as total and average commuting distances per individual, or modal split by distance class. Energy consumption data were also validated by feedback with values estimated by the regional energy agency for the whole territory. Finally, emissions produced by OLYMPUS for each class of emitters have been deeply compared and validated against reference inventories on the Paris region. For more details on the OLYMPUS operating principles and on the validation, please refer to Elessa Etuman and Coll (2018).

2.2. CHIMERE

Emission data from OLYMPUS are used as input in the Eulerian Chemical Transport Model (CTM) CHIMERE. The CHIMERE model, which constitutes the second block of the platform, has been used since the early 2000s by a wide community of stakeholders, both for regulatory and research purposes regarding air quality and atmospheric chemistry from the regional to the hemispheric scale (eg. Cholakian et al., 2021; Coll et al., 2009; Menut et al., 2020; Thunis et al., 2017). CHIMERE is regularly evaluated in the frame of its operational missions and has been part of several model intercomparison and model-observation comparison studies (Solazzo et al., 2012; Theobald et al., 2019; Ciarelli et al., 2019).

As a eulerian CTM, CHIMERE follows a deterministic approach integrating the evolution of pollutant concentrations over time and space for an area of interest. The area is first discretized into a 3D vertical grid of predefined resolution, which has been identified as relevant to the study of the target processes. Calculations are then performed in each mesh to reproduce the processes that apply to atmospheric species (either gaseous or size-resoled particulate species). These include emissions, chemical reactivity, deposition as well as transport and mixing processes induced by atmospheric dynamics. Regarding particulate matter, CHIMERE also considers nucleation, coagulation and gas absorption at the particle surface. In each grid cell of the domain, the calculation of atmospheric pollutant concentration levels is carried out on the principle of mass conservation, as presented below (Eq (1)):

$$\frac{\delta C_i}{\delta t} = \left(\frac{\delta C_i}{\delta t}\right)_{chemistry} + \left(\frac{\delta C_i}{\delta t}\right)_{transport} + \left(\frac{\delta C_i}{\delta t}\right)_{mixing} + \left(\frac{\delta C_i}{\delta t}\right)_{emissions} + \left(\frac{\delta C_i}{\delta t}\right)_{deposit} \quad (1)$$

For this study, we used the 2013 version of the model (see Menut et al., 2013 for more details), which proposes offline coupling with meteorological fields from weather forecasting models such as Weather Research and Forecasting (WRF), the European Centre for Medium-Range Weather Forecasts (ECMWF) or Météo France's global model ARPÈGE. The selected meteorological fields and derived turbulence parameters are projected and interpolated onto the simulation grid in a preprocessing step. In the standard CHIMERE configuration, anthropogenic emissions are expected in the form of gridded annual values per species. They also follow a pre-processing step which enables them to be redistributed on the simulation grid at the hourly step, and aggregated to match a selected chemical speciation if necessary. The model has been designed to handle data from the EMEP (Co-operative Programme for Monitoring and Evaluation of the Long-range Transmission of Air Pollutants in Europe, http://www.emep.int), TNO and Hemispheric Transport of Air Pollution (HTAP) (Janssens-Maenhout et al., 2015; Kuenen et al., 2014) emission programs. All of them provide information on the main gaseous pollutants such as non-methane volatile organic compounds (NMVOCs), nitrogen oxides (NOx), coarse and fine particles, carbon monoxide (CO), ammonia (NH_3) and sulfur oxides (SOx). Emissions are generally provided by sector of activity, according to a categorization compatible with the Standard Nomenclature for Air Pollution (SNAP, see Appendix A for more details). As for biogenic emissions, the Model of Emissions of Gases and Aerosols from Nature (MEGAN) from (Guenther et al., 2006) is implemented as a preprocessor. MEGAN calculates the emission factors of gaseous biogenic species per grid cell and per hourly time step according to landcover and meteorological conditions. Finally, CHIMERE displays a range of chemical schemes to describe the homogeneous reactivity of gas-phase species and their photolysis, as well as the formation and aging of the secondary organic aerosol (SOA). Both dry and wet deposition are considered. Dry deposition rates are conditioned by boundary layer meteorology and soil type, while wet deposition depends on the capture and dissolution of compounds present in clouds and rain droplets.

3. Configuration and input data

The modeling platform has been implemented for the Paris megacity, with 2009 as the base case scenario. There are two reasons for this choice. First, the validation of the OLYMPUS model was conducted for the year 2009 due to emission database availability. Second, the occurrence of notable air pollution episodes during the winter of that year: they provide contrasted situations of exposure to pollutants that are particularly relevant for mitigation studies. The simulation domain encompasses the entirety of the Parisian metropolis and contains 159 × 129 grid cells at a resolution of 1 km^2. This resolution aligns with the input data expected for the CHIMERE model. The administrative division adheres to the National Institute of Statistics and Economic Studies (INSEE) classification based, comprising 1300 zones called IRIS for the entire region. It is illustrated in Fig. 2 together with the simulation domain and all the nested domains necessary to run the CTM.

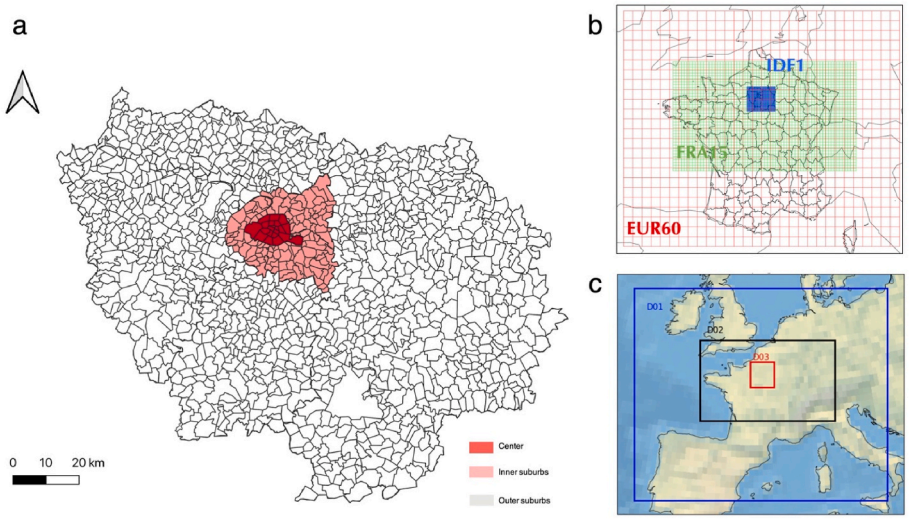

Fig. 2. Simulation domains and their resolution - Map a) represents the administrative division of the Ile de France region (Paris region), this division represents the 1300 IRIS defined following the National Institute of Statistics and Economic Studies (INSEE) classification. Map b) represents the different simulation domains and their nesting used in the CTM with increasingly refined resolution. Map (c) represents the different areas of weather forcing used as well as their nesting.

3.1. OLYMPUS setup

The synthetic population modeling setup relies primarily on regional population census data from INSEE (French National Institute for Statistics and Economic Studies) for the year 2009, with information available at the sub-municipality level. Using these data, we modeled the synthetic population based on distributions of household size, number of children per household, family types, employment rates and housing typologies (collective versus individual). Urban density index (UDI) threshold values for defining zone typology were derived from the observed population densities in French urban and rural areas (INSEE, 2015).

The mobility of urban population agents is configured from local transport survey data (EGT) (STIF, 2012) which serve as the basis for the modeling. They indeed are the basis for the calculation of attractiveness values for key activities, such as employment, school, leisure, and shopping. The average number of daily trips per agent in the synthetic population is based on the national household survey from (Armoogum et al., 2010). Public transport travel times stem from the analysis of the General Transit Feed Specification (GTFS) data for the Greater Paris area.

The energy demand configuration for buildings is informed by the local energy agency's statistics (ARENE, 2013) and national CEREN statistics (CEREN, 2015). These sources provide information on unit energy consumption per square meter and on the types of energy utilized by various housing types, including electricity, gas, wood, and district heating.

The configuration for modeling emissions from road transport and from combustion in residential and commercial sectors is based on Carteret et al. (2015) for vehicle fleet descriptions and CEREN data for heating/boiler systems in the residential and tertiary sectors.

3.2. CHIMERE setup

This study concentrates on the Paris metropolis, at a high resolution of 1 km^2. Since CHIMERE is a limited-area Eulerian model, it was necessary to constrain the concentrations at the simulation domain's boundaries by conducting nested simulations from a larger scale. To preserve information from the domain boundaries, we performed a triple nesting simulation, in which the largest domain EUROPE60 is constrained by climatological outputs from the global air quality model LMDZ-INCA. CHIMERE is run on this domain, at a horizontal resolution of 0.68° × 0.46°, and the output subsequently constrain the FRANCE15 national simulation domain which has a higher resolution of 0.205° × 0.135°. Finally, the national domain simulation outputs provide concentrations at the boundaries of the Paris domain (IDF1), which is the focus of our research. Fig. 2 provides a visualization of these simulation domains. Triple nesting allows a better representation of the various European contributions (e.g., large urbanized areas and the North Sea maritime corridor) to the air composition over the French territory during the study period. The decision to use an intermediary FRANCE15 domain aimed to capture the potential transport of air masses from the Ruhr region in Germany to Paris. The WRF model (Skamarock et al., 2008) was run as an offline meteorological forcing on all domains. Fig. 2 delineates the nested domain configuration.

The IDF1 domain, having the highest available resolution in CHIMERE (1 km^2), corresponds to the central area. Resolutions beyond this would entail a change in the nature of the processes and parameters determining air quality (local turbulence, buildings, etc.), thus necessitating the use of alternative models. This choice of a high-resolution domain, despite potentially lengthy computation times, is justified by the need to minimize error associated with modeling a highly heterogeneous urban environment. This choice is supported by the study of Colette et al. (2014) who compared PM_{10}, $PM_{2.5}$, and NO_2 concentration fields modeled by CHIMERE across three European domains with respective resolutions of 57 × 57 km^2, 8 × 8 km^2, and 2 × 2 km^2. Although the simulation period was brief (one winter week), the results showed a decrease in the error on the pollutant concentrations in urban environments as resolution increased. The IDF1 domain, forming a regular 1 km^2-resolution grid, spans the entire Paris metropolis across the longitude interval [1.457°–3.606°] W and the latitude range [48.10°–49.25°] N. Horizontally, the domain is divided into 20,511 grid cells. Vertically, eight levels are delimited between ground pressure and 750 hPa, corresponding to CHIMERE's optimal configuration for flat terrain applications at this scale.

Regarding emissions for the two large-scale simulations, we opted for the European EMEP inventory with a spatial resolution of 0.25°, widely used in CHIMERE's national-to-continental simulations. For the main simulation, we employed OLYMPUS emissions that were provided at a resolution of 1 km^2, after combining them with inventories containing complementary emissions. We notably used the reference local emission inventory from the Paris air quality monitoring agency AIRPARIF, which allows to consider the industrial emissions on the region. The detailed procedure is shown in (Appendix C). For biogenic emissions, we retained

a standard configuration using the MEGAN model for all domains.

To enable this simulation to be evaluated, we have simultaneously carried out a simulation that is identical in every respect, but which uses all the tabulated emissions supplied by the AIRPARIF reference inventory in the IDF1 domain, instead of the OLYMPUS data. This referent simulation therefore contains the state of the art in terms of modeling traffic emissions and energy use in buildings: comparing the outputs of these 2 simulations will enable us to assess the quality of the data produced by OLYMPUS-CHIMERE.

4. Results and discussion

In this section, we present the results provided by the modeling chain for simulating air quality in the Paris region. Their relevance is discussed on the basis of their comparison with measurements from the air quality network AIRPARIF, and with our reference simulation carried out with the AIRPARIF reference inventory data. Several summary figures are presented in this section, and additional figures and tables can be found in Appendix D.

4.1. OLYMPUS-CHIMERE outputs

Fig. 3 shows a series of cartographic representations of the data produced by our platform, for the Paris region and in the configuration described above. Emission maps from OLYMPUS, for subsets of emitters, are shown in the left-hand column. Interpolated concentration maps of mean annual values for the main atmospheric species of interest are shown in the right-hand column.

Fig. 3 well highlights the linearity of road transport emissions compared with the surface component of emissions related to population density. The gradient of emissions linked to building use reveals the centric nature of the Paris region, which is organized around the densely populated urban center that is the city of Paris. This center is surrounded by a first ring of outlying communes (inner suburbs), presenting also a marked urban character. Communes in the outer suburbs of Paris have a more spread-out layout and a pronounced rural and agricultural character. Paris and its inner suburbs are served by a high-density road network. This network supports significant commuting activity towards the center every day, with roads being heavily trafficked and even subject to recurrent congestion, as can be seen in the intensity of all road-related emissions. These are well-known features for the Paris region, and their presence in the emission data confirms the comprehensive nature of the OLYMPUS simulation. The main limitations of the model in its current version are the lack of consideration for travels from outside city limits, and the underestimation of the transport of goods. The model's ability to reproduce a relevant emission situation in space and time is more deeply discussed in Elessa Etuman and Coll (2018).

The concentration maps in Fig. 3 logically show concentration gradients of primary species (directly emitted into the atmosphere) with increasing concentrations towards the center of the region. This character is strongly marked for nitrogen dioxide (NO_2), due to the intensity of its combustion-related urban sources and its short lifetime. Nitrogen oxides are indeed rapidly converted into nitric acid or in the form of organic nitrates. Conversely, high levels of nitrogen oxides in the center of the region lead to a consumption of ozone that is characteristic of urban areas. For particulate matter, the shape of the average concentration fields reflects a lesser spatial dependence on emission gradients. This is due to the fact that particles persist longer in the atmosphere and mixing with the regional atmosphere is less effective in lowering levels.

Fig. 4 represents the hourly concentration distribution of the same four pollutants, divided across three areas: central Paris (black), inner suburbs (grey), and outer suburbs reaching the Île-de-France region's

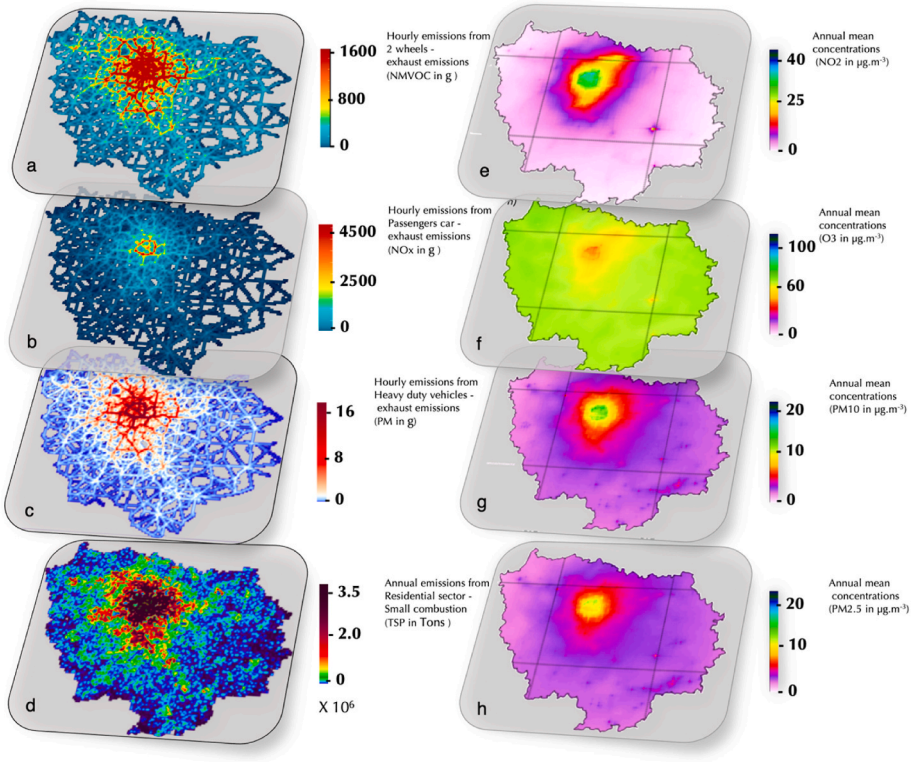

Fig. 3. Examples of outputs of the OLYMPUS-CHIMERE modeling chain. The maps a), b) c) and d) represent respectively emissions of volatile organic compounds related to the escape of 2 motorized wheels, nitrogen oxides of private vehicles, emissions of fine particles related to the exhaust of heavy trucks and combustion-related particulate emissions in the residential sector. The emission maps (a), (b), and (c) represent hourly emission values and map (d) represents annual emission values. Maps (e), (f), (g) and (h) represent the annual average of concentrations of nitrogen dioxide, ozone, particles smaller than 10 μm in diameter and fine particles less than 2.5 μm.

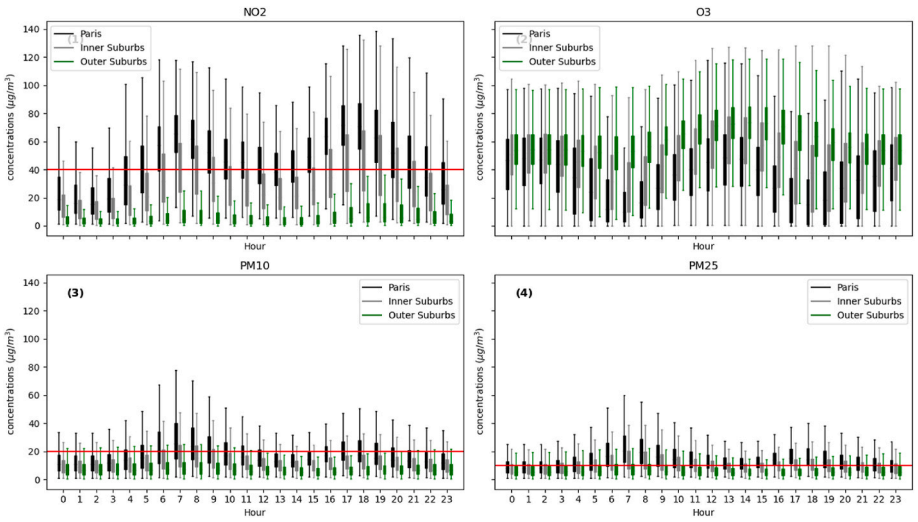

Fig. 4. Boxplot time series of average hourly values of NO_2, O_3, PM_{10} and $PM_{2.5}$ ($\mu g.m^{-3}$) modeled by area by OLYMPUS-CHIMERE. In black concentrations in the city center, in grey concentrations in the inner suburbs and in green concentrations in the outer suburbs - red lines represent WHO regulatory/recommendation thresholds.

boundaries (green). The 24 boxplots deliver the concentrations simulated for each hour of every 2009 day, for each domain grid point. Each boxplot's value distribution thus arises from spatial disparities within a region as well as day-to-day fluctuations. This figure shows the growth in concentration variability as we get closer to the urban heart. Such a diurnal pattern emerges from both dynamic atmospheric boundary layer influences and emission dynamics.

OLYMPUS-CHIMERE's projections, in line with current urban air quality understanding, highlight an increasing spatiotemporal NO_2 concentrations variability from the outer suburban zones to the metropolitan core. For our study, the median concentrations during each hour (depicted as the box center) surpass the WHO's health protection threshold (40 µg/m3) throughout the 7 a.m. to 8 p.m. timeframe. Evening and nighttime concentrations are noticeably lower and more consistent across the region. It is pertinent to note that our simulations utilize a kilometer-scale resolution and are driven by a mesoscale CTM, which doesn't account for pollution confinement by buildings, such as in heavily-trafficked narrow streets bordered by structures. Thus, the results more closely represent average urban pollution, offering a conservative estimate for residents' exposure near major roads. The CTM's potential underrepresentation of fine-scale air pollution might also impact less urbanized zones. Spatial averaging in these areas often erases the near-road pollution signature, so the green value distribution may not reflect actual urban and outer suburban conditions. This is an intrinsic CTM limitation.

The spatial disparities and daily particulate matter concentration shifts are analogous to those of NO_2 but are less pronounced. Peak traffic times in the two central areas still witness elevated percentiles, albeit to a reduced degree. In terms of health guideline compliance, our model forecasts concentration values in the city center that breach WHO recommendations for PM_{10} and $PM_{2.5}$, at 20 µg/m3 and 10 µg/m3, respectively. Like NO_2, these represent urban background concentrations and do not consider traffic-proximate exposure.

Lastly, OLYMPUS-CHIMERE predicts a more subdued ozone gradient, with sharper depletion and a heightened daily cycle in the nitrogen oxide-rich urban core. Such characteristics are anticipated for ozone concentration patterns.

4.2. Evaluation of OLYMPUS-CHIMERE outputs

The air quality climatology of large metropolises, such as Greater Paris, has been extensively recorded through measurements and modeling. The aforementioned figures are crucial as they validate our platform's capability to reproduce the well-known spatial and temporal primary pollutant concentration variability by statistically diagnosing activity and mobility in the metropolis. In the subsequent section, we focus on the quantitative assessment of the absolute values and concentration gradients simulated by OLYMPUS-CHIMERE.

The aim of this comparison work is to evaluate the OLYMPUS-CHIMERE integrated modeling chain not only in terms of the concentrations generated, but also in terms of its ability to recreate the main characteristics of concentrations trends over an area and over time. As we announced above, the validation work is based on the comparison of output data from the OLYMPUS-CHIMERE platform with an AIRPARIF-CHIMERE simulation based on a state-of-the-art inventory used for regulatory air quality missions, and with measurement data.

To measure the importance of the model intercomparison work, it should be pointed out that the emission sectors modeled by OLYMPUS represent, according to AIRPARIF estimates for the Paris region, 75% of total nitrogen oxide emissions, and 50% and 60% of total PM_{10} and $PM_{2.5}$ emissions respectively. The pollutant emissions derived from the OLYMPUS model were validated in accordance with the methodology established in the study by Elessa Etuman and Coll (2018). This validation procedure was conducted in several phases, at each step of the production of output data, to verify the model's ability to replicate the reference scenario characteristics. It is worth noting that, compared to the model's initial version, the emission calculation methodology has been updated, transitioning from COPERT 4 to COPERT 5. Additionally, the traffic modeling within OLYMPUS has been optimized to better capture congestion phenomena. Based on the cadastral data from the reference year, the model estimates increased emissions, notably for NOx, with a rise of 20% for all the transportation sector, 11% for passenger car exhaust emissions for NO_x, over 40% for fine particles from exhaust emissions and 8% for NMVOCs. Discrepancies in emission inventories have been described in the litterature. We can refer to the work of (Timmermans et al., 2013) on the sensitivity of urban air quality to emissions inventories, which indicates that although inventories may rely on common approaches such as COPERT, assumptions on the vehicle fleet or parameterizations of cold-road fractions, for example, can justify a minimum of 20% deviation on emission totals. In our case, we also need to consider assumptions relating to congestion modeling, average speed per road segment and lane occupancy by light and heavy duty vehicles.

Fig. 5 has been set up to assess the differences in concentrations

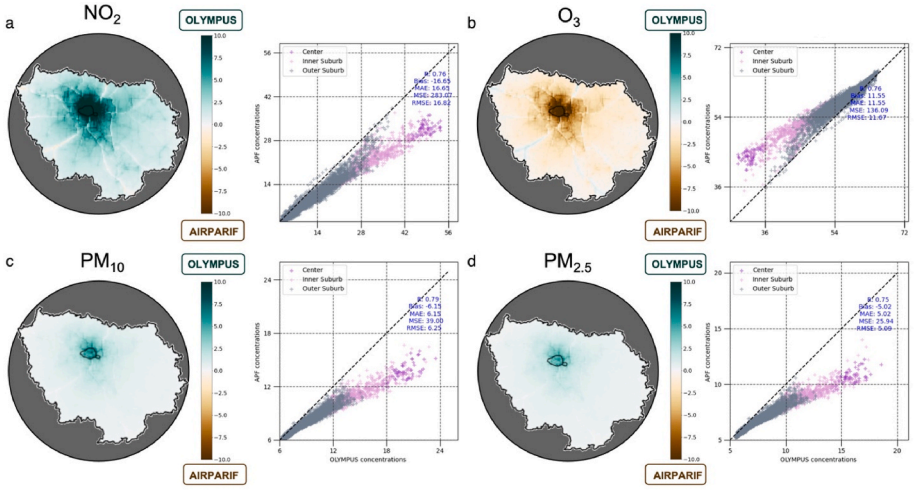

Fig. 5. Comparison with a conventional emissions inventory. Figures a), b), c) and d) represent concentration difference maps from annual averages between the 2 simulations respectively for NO_2, O3, PM_{10} and $PM_{2.5}$ ($\mu g.m^{-3}$).

induced by the differences in the emission calculation methods between OLYMPUS and the AIRPARIF reference inventory. In the circles, we have mapped the differences (in $\mu g/m^3$) in the mean annual concentrations of NO_2 (top left), ozone (top right), PM_{10} (bottom left) and $PM_{2.5}$ (bottom right). Differences are calculated in the [OLYMPUS-CHIMERE] - [AIRPARIF-CHIMERE] direction. They are colored green when the OLYMPUS-CHIMERE model gives higher concentration values, and conversely. To the right of each circle, we have plotted average annual concentrations in each grid cell from the reference simulation (Y-axis) against concentrations from the OLYMPUS-CHIMERE simulation (X-axis), using a color code to distinguish the spatial origins of the concentration dots. Three zones are made up: central Paris is in purple, the densely urbanized inner suburbs are in pink, and the outer suburbs are in grey.

For all species and all domains in Fig. 5, the data from the two simulations appear highly consistent with each other, with concentration levels showing a strong linear correlation. This is quite important, as this linearity confirms that the OLYMPUS-CHIMERE model does indeed reproduce the spatial concentration gradient over the region, and hence the territorial distribution of emission zones. In the specific case of NO_2, since the share of emissions from OLYMPUS is around 75%, we can consider that the small common fraction of emissions between the two simulations is not the main reason for their very high consistency, which is therefore attributable to a relevant distribution of emitting activities by OLYMPUS over the region.

It should be noted, however, that for all primary species (NO_2 and particulate matter) the slope of the correlation line is significantly lower than 1, which (all other parameters being equal) indicates a tendency for OLYMPUS to propose more intense emissions than the reference inventory in the dense urban center. This discrepancy is not problematic, as it results from different sets of hypotheses and input data. The maps in Fig. 5 provide a more detailed representation of the spatial distribution in the model differences, which increase with proximity to the densely populated and heavy road traffic central areas (green colors). In the case of NO_2, they reach up to $+10$ $\mu g/m^3$ in OLYMPUS-CHIMERE over the entire central and inner suburbs of Paris. The spatial extent of this phenomenon is smaller for fine particulates, and essentially limited to Paris and neighboring municipalities, with differences of up to $+5$ $\mu g/m3$ for OLYMPUS-AIRPARIF and on major roads.

Several points (in grey) escape this trend. They are mainly visible for NO_2 (although this trend also exists for particulate matter) and are - this time - aligned with the slope 1 line. On the map of model differences, we can see that they correspond to major traffic roads linking the urban center to neighboring regions. We believe this phenomenon in outers suburbs may be due to a lack of volume in suburban highway emissions, which can be at least partly attributed to the share of interregional transport and freight, which is not coded in the motives for mobility in OLYMPUS. However, a lack of assignment of commuting on the road network in the outer suburbs cannot be completely ruled out. The tables with the statistical analysis of simulated versus measured data are presented in Appendix D. They show that the scores and quality of the two simulations are very similar.

4.3. Exposure derived from simulation data

To complete the work, we estimated population exposure using outputs from the 2 model configurations. The exposure parameter is called *EXPO* and it can be estimated from any of the four pollutants we displayed in our study. *EXPO* was calculated across distinct urban regions, namely the center, inner suburbs, and outer suburbs. This quantification was achieved by intersecting high-resolution population density maps - derived from census data - with annual mean pollutant concentration maps from CHIMERE. The equation for exposure is defined as:

$$EXPO(i) = \frac{\sum_{agent} Exposure(agent, i)}{n_{Agents}}$$

Where.

$EXPO(i)$ denotes the mean exposure of the population within area *i*.
$Exposure(agent, i)$ represents the exposure experienced by a specific agent in the area *i*.
n_{Agents} is the total count of modeled agents, assessed within the specified area *i*.

In essence, the equation computes the average pollutant exposure within a given urban region *i* by accumulating the exposure levels of all individual agents, and normalizing by the total number of agents. Through this methodology, we were able to provide a classic assessment of population-centric exposure levels across different urban gradients. The results are presented in Fig. 7 for NO2 (top left), ozone O_3 (bottom left), and fine particles (top right for PM10 and bottom right for PM2.5). The histograms show the cumulative EXPO value obtained from the reference configuration (in red) and the OLYMPUS configuration (in black) for each of the 3 sub-domains of our study. The surface charts display the frequency of individual exposures with OLYMPUS emissions (in grey) and the reference AIRPAPRIF emissions (in light red).

Fig. 6 illustrates the differences previously observed between

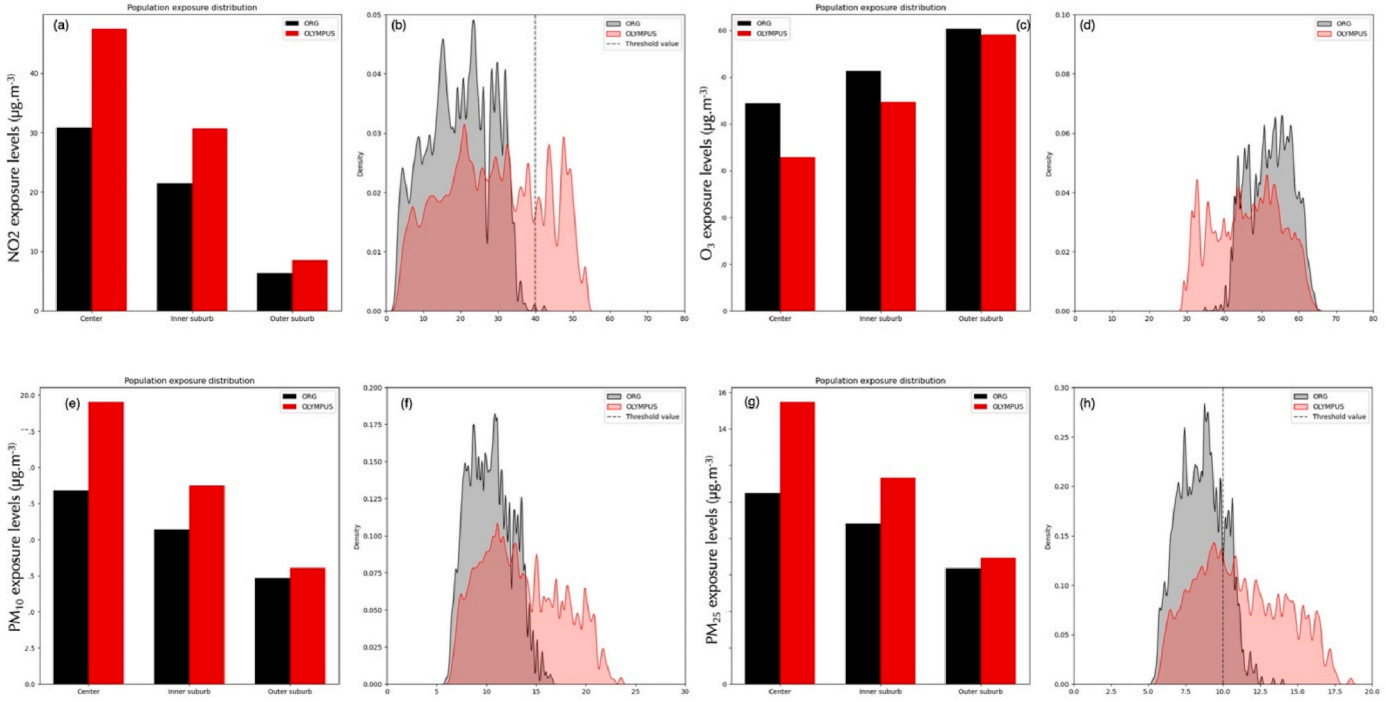

Fig. 6. Representation of the population exposure. Figures (a), (c), (e) and (g) represent mean values of population exposure by place of residence respectively for NO_2, PM_{10}, O_3 and $PM_{2.5}$. Figures (b), (d), (f), and (h) display the distribution of population fractions along their average exposure level on the x-axis. Specifically, figure (b) represents exposure to NO_2, figure (f) to O_3, figure (d) to PM_{10}, and figure (h) to $PM_{2.5}$.

simulations, i.e. higher concentrations of primary pollutants in the dense zone in the modeling configuration using the OLYMPUS inventory. However, the frequency distribution of exposures highlights a new element: the effect of massive exposure, linked to the fact that a very large proportion of the Paris region population lives in the dense urban areas of the metropolitan center. Thus, for NO_2, and even for fine particles for which the differences between the simulations were observed over a very small area of the domain, the differences in exposure concern a very large part of the colored surface on the frequency graphs. A very large proportion of the population is therefore affected by exposure in dense areas, and this proportion would even increase if we were to take into account people commuting towards Paris during the day. This observation calls for two comments. Firstly, it appears is essential to refine our spatial representation of air quality in dense urban areas, as it is a key parameter for population exposure. That is why further steps to refine CHIMERE output data need to be considered. Secondly, the use of a tool like OLYMPUS in forcing CHIMERE makes a great deal of sense, since it enables us to better understand the link between urban organization, mobility practices and emissions, which drive most of the population exposure in metropolitan areas.

5. Conclusions

In this article, we have carried out a detailed analysis of the results produced by an innovative air quality modeling platform coupling an emission model (OLYMPUS) with a chemical transport model (CHIMERE). The innovative aspect of this platform lies in the use of OLYMPUS to produce a set of emissions based on a statistical representation of the population's activities. Modeling in OLYMPUS is initiated by the creation of a realistic synthetic population based on survey data. The model then produces all the parameters determining mobility locations, modes, motives, and agendas, as well as the parameters related to energy consumption in buildings. The modeling process ends as OLYMPUS produces a spatialized emission inventory resulting from its analysis of the territory and the population's practices. This inventory is used as input data for the CHIMERE air quality simulation. As OLYMPUS outputs were evaluated in a previous work, we evaluated here the air quality data. Our simulation was carried out for the Greater Paris region, for the year 2009. In this validation work, we demonstrated the ability of the OLYMPUS-CHIMERE platform to produce a comprehensive representation of the concentration gradients of the main primary pollutants over the domain of interest (NO_2, PM_{10}, $PM_{2.5}$ mainly), and of the variability of these concentrations. We were able to compare our results with those of a simulation carried out with an emissions inventory corresponding to the state of the art in bottom-up inventories. We observed two main differences in the output concentration fields. First, higher concentration values for primary pollutants in the dense zone were produced by OLYMPUS, but this difference remains compatible with differences in inventory methodology and it even brings some improvements in the concentration fields. On the other hand, we saw that road transport on a few major regional routes may be underestimated, mainly because OLYMPUS in this version does not integrate inter-regional mobility and possibly due to an underestimation of freight transport. Changes in the parameterization of the OLYMPUS module for inter-regional transport, FRET, should be considered. Comparison with data from the local air quality network finally showed that our results are fully comparable with simulations carried out with state-of-the-art inventories, and even allowed for NO_2 concentration improvements in the metropolis. Finally, observing the distribution of exposures across the domain of study highlighted the importance of refining our understanding of the links between urban configuration, housing, mobility, transport and emissions in metropolises. Indeed, since metropolises are densely populated areas, small differences in pollution levels in their center lead to great differences in total exposure, which may raise major public health issues.

As a conclusion, our study allows to validate air quality modeling using the OLYMPUS-CHIMERE platform, in terms of spatial and temporal distribution of pollutant concentrations over the Paris metropolis but also by comparison with well-acknowledged emission data. In the future, the OLYMPUS-CHIMERE platform will be dedicated to the analysis of new urban scenarios involving changes in urban planning or individual mobility behaviors. The validation of our results provides the

OLYMPUS-CHIMERE coupling with a reliable framework to produce air quality diagnostics in prospective situations and for addressing research questions linked to the impact of urban policies on air quality.

Still, these works open up new development and application prospects. Air quality modeling with CTMs needs to be enriched by further steps to refine their diagnosis of urban air quality. This shortcoming becomes evident particularly when considering intricate urban parameters, such as the complex interplay of the urban morphology - which considers spatial arrangements and typologies of built forms - and the very local gradients of emissions. To enhance the predictive capability of CTMs, the issues of fine-scale representativeness must be addressed. Implementing potential corrections derived from a profound understanding of the immediate environment might be the key. These could be sourced from a range of methodologies, whether statistical and drawing from established patterns; empirical and based on direct observation or experience; or deterministic and rooted in fundamental cause-and-effect paradigms.

CRediT authorship contribution statement

Arthur Elessa Etuman: Formal analysis, Data curation, designed, conceived, and implemented the entire model. performed the model and analyzed data. **Isabelle Coll:** Writing – original draft, coordinated the study. Wrote the paper: AEE & IC.

Declaration of competing interest

The authors declare that they have no known competing financial interests or personal relationships that could have appeared to influence the work reported in this paper.

Data availability

Data will be made available on request.

Acknowledgements

This work was performed using HPC resources from GENCI-CCRT (grant 2017-t2015017232). This work received support from the French National Agency for Research (ANR-14-CE22-0013) and the Île-de-France region (DIM R2DS). We also acknowledge AIRPARIF and the LABEX Urban Futures.

Appendix

Appendix A. Selected Nomenclature for Air Pollution (SNAP)

Emission inventories are based on SNAP (Nomenclature for Air Pollution Nomenclature, EMEP/CORINAIR, 1997).
SNAP Code – Description.

01 Combustion in the production and transformation of energy
02 Non-industrial combustion plants
  02 01 Commercial and institutional plants
  02 02 Residential plants
  02 03 Plants in agriculture, forestry and aquaculture
03 Industrial combustion plants
04 Industrial processes without combustion
05 Extraction and distribution of fossil fuels and geothermal energy
06 Use of solvents and other products
07 Road Transport
  07 01 Passenger cars
  07 02 Light duty vehicles <3.5 t
  07 03 Heavy duty vehicles >3.5 t and buses
  07 04 Mopeds and Motorcycles <50 cm^3
  07 05 Motorcycles >50 cm^3
  07 06 Gasoline evaporation from vehicles
  07 07 Automobile tyre and brake wear
08 Other mobile sources and machinery
09 Waste treatment and disposal
10 Agriculture
11 Other sources and sinks (nature)

Appendix B. Statistical tools

As part of the model/measure comparison, the estimated value corresponds to the modeled value (i) (mi) and the reference value corresponds to the value observed by the measure (oi).

Mean Bias (***MB***)

$$\boldsymbol{MB} = \frac{1}{n}\sum_{i=1}^{n}(mod_i - obs_i)$$

Normalized Mean Bias (***NMB***)

$$\boldsymbol{NMB} = \frac{\frac{1}{n}\sum_{i=1}^{n}(mod_i - obs_i)}{\overline{obs}}$$

Root Mean Square Error(***RMSE***)

$$\boldsymbol{RMSE} = \sqrt{\frac{1}{n}\sum_{i=1}^{n}(mod_i - obs_i)^2}$$

Normalized Root Mean Square Error (***NRMSE***)

$$\boldsymbol{NRMSE} = \frac{\sqrt{\frac{1}{n}\sum_{i=1}^{n}(mod_i - obs_i)^2}}{\overline{obs}}$$

Pearson correlation coefficient (***R***)

$$\boldsymbol{R} = \frac{\sum_{i=1}^{n}(mod_i - \overline{mod})(obs_i - \overline{obs})}{\sqrt{\sum_{i=1}^{n}(mod_i - \overline{mod})^2 obs_i - \overline{obs}}}$$

Appendix C. OLYMPUS-CHIMERE emissions post-processing

In the current version of OLYMPUS, only road transport emissions (SNAP code 07) and combustion emissions in the residential/institutional/commercial sector (SNAP code 02) are modeled, as they correspond to our representation of people's daily activity. To take into account all CHIMERE's input emitting sectors and produce a realistic simulation, it was necessary to integrate additional emissions. OLYMPUS emissions have thus been associated with emissions from the S1, S3, S4, S5, S6, S8, S9 and S10 sectors of the SNAP classification, all gathered from the bottom-up reference emission inventory produced by the local air quality monitoring agency AIRPARIF. These emissions notably stem from the industrial sector, whether point emissions from large combustion plants or surface emissions, such as those from manufacturing industries.

However, while our rectangular domain IDF1 contains areas outside the Île-de-France region at its corners, AIRPARIF emissions do not cover areas outside the Paris administrative region. We therefore also aggregated emission data from the EMEP top-down inventory on these external zones, to ensure complete coverage of the CTM simulation domain.

Fig. 7 shows a schematic of the processes used to treat emissions and associate the OLYMPUS model with the emissions of bottom-up and top-down emissions inventories.

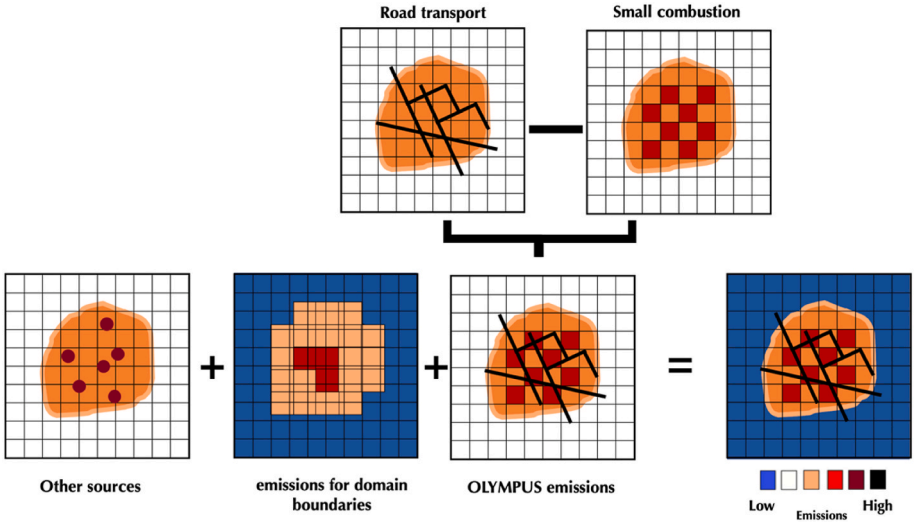

Fig. 7. preprocessing of anthropogenic pollutant emissions from the OLYMPUS model

Appendix D. Comparison of model predictions with measurements

D.1. AIRPARIF monitoring network.

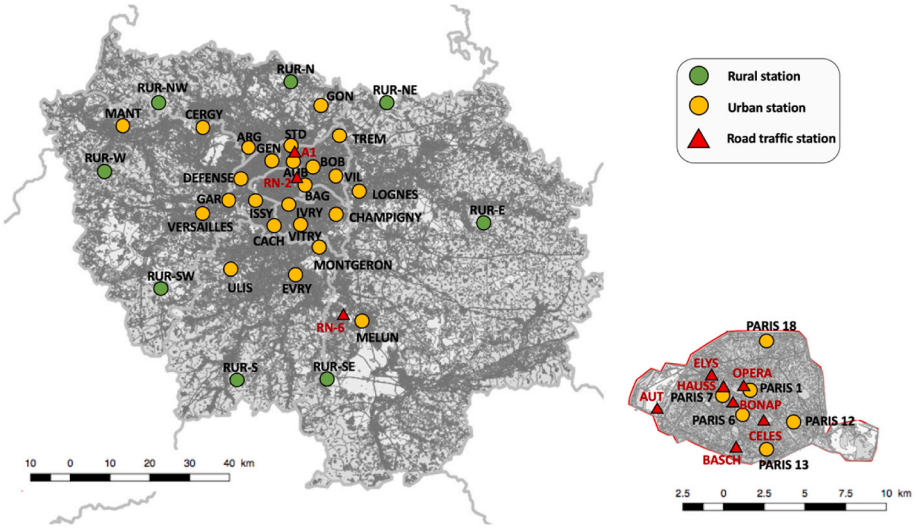

Fig. 8. Measuring network of permanent stations of AIRPARIF - The rural stations are represented by green pellets, the urban bottom station by yellow pellets, the stations of traffic by red triangles. - Map b) represents the RMSE difference observed for the measurement stations of the AIRPARIF network between the two simulations.

The AIRPARIF station network, created in 1979, is responsible for monitoring air quality throughout the entire Paris region. This AASQA has a network of 64 measurement stations, including 51 permanent stations. The purpose of the spatial distribution of these stations is to quantify the exposure in the urban background but also in proximity to the transmitters (industrial, road in particular). The so-called "traffic" stations aim to approach the values of immediate exposure to vehicle emissions. These stations can be positioned in the city center, at the edge of the tracks or on a sidewalk, or close to major road infrastructures. The distance to traffic is standardized, it depends on the average daily rate of vehicles passing on the track. The base stations are more distant from local traffic and measure the average levels of pollution of a more homogeneous area. In the measurement network of AIRPARIF there are 3 types of base stations. Urban, peri-urban, and rural bottom stations. The measurement of ozone is made by absorption of ultraviolet radiation, that of NOx by chemiluminescence and the masses of fine particles taken from the air are measured by TEOM-FDMS analyzers. The stations available for the study are presented by site typology in Fig. 9. Our model-measure comparison is supported by standard statistical tools for assessing the gaps between the two datasets. We compared the concentration fields modeled by the OLYMPUS-CHIMERE platform with measurement data from the regulatory air quality monitoring network implemented by AIRPARIF (here named MES-APF). Our objective is the differentiated analysis between the signals of modeled concentrations and the measurements obtained on different types of measurement sites.

Table. 1
Comparative analysis of observed versus simulated concentrations and the associated statistical metrics for several pollutants and multiple measurement stations (units are $\mu g/m^3$)

NAMES	RMSE		MB		NMB		NRMSE	
	OLYMPUS	ORG	OLYMPUS	ORG	OLYMPUS	ORG	OLYMPUS	ORG
NO_2								
AUB	21.58	19.77	3.59	−5.88	8.43	−13.79	50.64	46.39
BAGN	23.81	19.93	6.77	−4.17	17.15	−10.57	60.32	50.49
BOB	22.27	21.18	6.06	0.46	18.04	1.36	66.27	63.03
CACH	24.81	25.18	6.85	6.34	19.89	18.42	72.06	73.12
CERGY	14.85	15.73	−6.55	−6.51	−33.02	−32.82	74.92	79.35
CHAMP	20.16	20.43	−1.04	−5.36	−3.38	−17.47	65.75	66.63
DEF	18.54	16.74	4.79	−0.34	13.38	−0.96	51.83	46.79
EVRY	17.85	19.31	−6.49	−12.19	−23.06	−43.33	63.44	68.63
GARCH	17.23	16.83	0.54	1.78	2.29	7.47	72.3	70.64
GEN	19.59	20.74	−1.1	−2.58	−2.93	−6.9	52.28	55.36
GON	19.84	19.17	7.45	5.7	27.21	20.79	72.41	69.99
ISSY	19.76	19.66	−1.35	2.3	−3.74	6.36	54.62	54.35
IVRY	27.03	21.14	11.72	0.67	33.19	1.88	76.53	59.84
LOGNES	20.16	21.44	−9.92	−13.19	−31.59	−41.99	64.18	68.23
MANT	19.11	20.52	−13.66	−15.71	−61.4	−70.63	85.89	92.23
MELUN	17.71	20.48	−13.43	−17.7	−51.97	−68.47	68.53	79.23
MONTG	16.91	18.08	−5.13	−8.75	−19.16	−32.65	63.12	67.48
NEUIL	26.81	24.01	11.57	7.11	28.73	17.67	66.61	59.65
NOGENT	22.41	23.06	0.27	−9.42	0.75	−25.92	61.67	63.45
PA06	24.7	25.69	11.29	11.37	31.36	31.59	68.6	71.36
PA07	19.87	21.85	2.61	5.37	6.21	12.8	47.37	52.1
PA12	24.55	21.3	6.98	−2.65	16.49	−6.26	58.01	50.33
PA13	23.27	21.61	8.07	4.28	21.03	11.14	60.6	56.28
PA18	21.81	22.47	4.04	0.34	8.99	0.75	48.54	50.01
STDEN	20.21	19.91	−0.13	−7.28	−0.33	−18.81	52.21	51.45
TREMB	18.96	19.24	−5.45	−8.25	−17.77	−26.92	61.85	62.77
VERS	16.63	15.98	−6.54	−6.67	−23.97	−24.43	60.93	58.54

(*continued on next page*)

Table. 1 (*continued*)

NAMES	RMSE		MB		NMB		NRMSE	
	OLYMPUS	ORG	OLYMPUS	ORG	OLYMPUS	ORG	OLYMPUS	ORG
VILLEM	20.31	20.33	−1.3	−7.99	−3.99	−24.44	62.1	62.18
VITRY	21.6	21.87	−4.99	−7.77	−13.43	−20.93	58.17	58.9
PM_{10}								
BOB	19.83	22.21	−13.2	−17.91	−44.34	−60.15	66.61	74.58
GEN	19.36	21.34	−13.16	−16.98	−45.28	−58.44	66.64	73.46
GON	18.9	19.94	−14.42	−16.31	−52.38	−59.27	68.65	72.42
PA01H	19.61	20.21	−7.26	−15.1	−24.95	−51.88	67.39	69.47
VITRY	18.79	20.69	−13.55	−16.67	−49.71	−61.18	68.96	75.92
$PM_{2.5}$								
GEN	12.34	12.89	−5.7	−8.26	−30.43	−44.04	65.84	68.78
PA01H	12.76	12.5	−3.26	−8.74	−15.57	−41.72	60.91	59.7

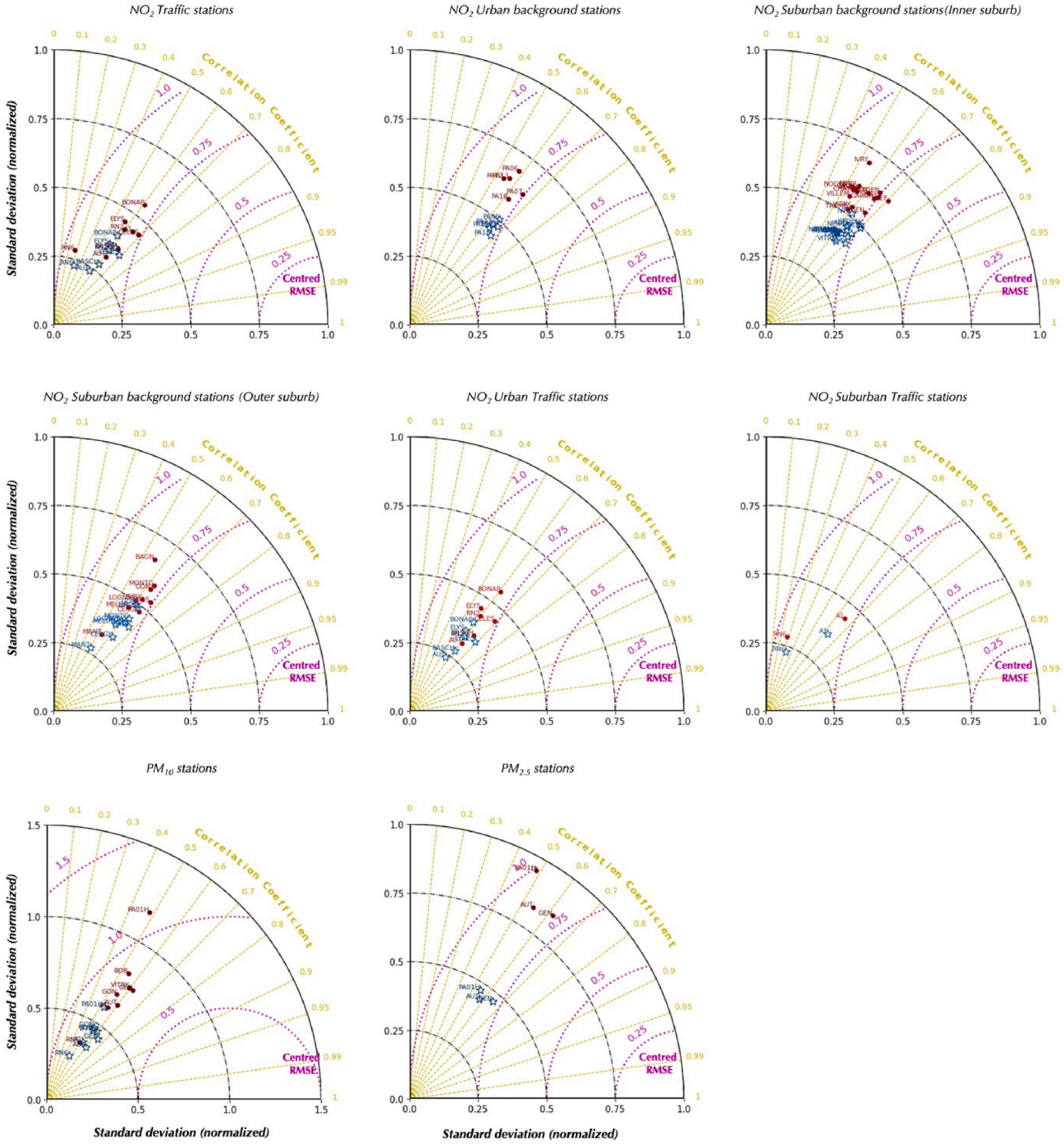

Fig. 9. Taylor Plots of scores from modeled hourly NO_2 PM_{10} and $PM_{2.5}$ in the Ile-de-France Region with the OLYMPUS-CHIMERE platform (red dots) and with the reference AIRPARIF-CHIMERE configuration (blue stars). Dotted purple lines account for centered RMSE, dotted yellow lines for the correlation coefficient, and dotted black lines for normalized standard deviation. Measurement data are from AIRPARIF's permanent stations for year 2009.

We also looked deeply in statistically at the differences between the different simulations using a Taylor diagram for NO_2 and fine particles based on Monteiro et al. (2018) methodology (Fig. 9). Within the metropolitan area of Paris, encompassing central Paris, the inner suburbs, and the outer suburbs, we performed a speciation based on the typology of the measurement stations. We did this for several types of measurement stations (background and traffic stations) and by territory (Paris, suburbs, rural areas). The Taylor diagram elucidates the distribution of simulation scores achieved with the two different model configurations, in comparison with the data collected from measurement stations. The diagram displays the correlation index, normalized standard deviation, and Root Mean Square Error (RMSE) at each station. The principle consists in positioning a point representative of the scores of a simulation in a plane. The centered Root Mean Square Error (RMSE) of the models can be read on the dotted purple curved lines. Correlation coefficients are displayed on the dotted yellow lines. Normalized standard deviation is the ratio between the variance of the

model data versus that of the observations. Its values can be read on the dotted black curved lines. In the Taylor Plot presented here, the comparison between the observed and predicted air pollutant concentrations for the Ile-de-France Region is conducted using hourly concentrations. OLYMPUS-CHIMERE simulation scores are depicted by red dots, while that of AIRPARIF-CHIMERE are shown as blue stars.

The distribution of the points representative of the simulations is similar in all configurations. The red points are always located a little further up and to the right of the blue stars, which means that the OYMPUS-CHIMERE configuration achieves slightly better scores, linked to a more complete restitution of the hourly data amplitude and to a slightly reduced RMSE. Correlation scores do not show significant differences between the simulation, not least because the results depend on common forcings, such as the hourly distribution of emissions and atmospheric dynamics at ground level. The new inventory thus brings improvements in the simulation, but the scores do not present a drastic departure from the old ones. These results validate the approach implemented in OLYMPUS-CHIMERE, its applicability, and its robustness on the domain.

References

Airparif, 2013. Bilan des émissions de polluants atmosphériques et de gaz à effet de serre en Ile-de-France pour l'année 2010 et historique 2000/2005.

ARENE, 2013. La Facture Énergétique Francilienne (Paris, France).

Armoogum, J., Bouffard-Savary, É., Caenen, Y., Couderc, C., Courel, J., Delisle, F., Duprat, P., Fouin, L., François, D., Gascon, M.-O., Godineau, D., Grimal, R., Hubert, J.-P., Gal, Y., Le, L.J., Verry, D., 2010. La mobilité des Français, panorama issue de l'enquête nationale transports et déplacements 2008.

Carteret, M., Andre, M., Pasquier, A., 2015. Méthode d'estimation des parcs automobiles et de l'impact de mesures de restriction d'accès sur les émissions de polluants.

CEREN, 2015. Données statistiques du CEREN, pp. 1–32.

Ciarelli, G., Theobald, M.R., Vivanco, M.G., Beekmann, M., Aas, W., Andersson, C., Bergstrom, R., Manders-Groot, A., Couvidat, F., Mircea, M., Tsyro, S., Fagerli, H., Mar, K., Raffort, V., Roustan, Y., Pay, M.-T., Schaap, M., Kranenburg, R., Adani, M., Briganti, G., Cappelletti, A., D'Isidoro, M., Cuvelier, C., Cholakian, A., Bessagnet, B., Wind, P., Colette, A., 2019. Trends of inorganic and organic aerosols and precursor gases in Europe: insights from the EURODELTA multi-model experiment over the 1990-2010 period. Geosci. Model Dev. (GMD) 12, 4923–4954. https://doi.org/10.5194/gmd-12-4923-2019.

CITEPA, 2014. Rapport national d'inventaire Inventaire des émissions de polluants atmosphériques et de gaz à effet de serre en France – Séries sectorielles et analyses étendues.

Cholakian, A., Coll, I., Colette, A., Beekmann, M., 2021. Exposure of the population of southern France to air pollutants in future climate case studies. Atmos. Environ. 264, 118689, 2021.

Colette, A., Bessagnet, B., Meleux, F., Terrenoire, E., Rou??l, L., 2014. Frontiers in air quality modelling. Geosci. Model Dev. (GMD) 7, 203–210. https://doi.org/10.5194/gmd-7-203-2014.

Coll, I., Lasry, F., Fayet, S., Armengaud, A., Vautard, R., 2009. Simulation and evaluation of 2010 emission control scenarios in a Mediterranean area. Atmos. Environ. 43 (27), 4194–4204.

Elessa Etuman, A., Coll, I., 2018. OLYMPUS V1 . 0 : Development of an Integrated Air Pollutant and GHG Urban Emissions Model – Methodology and Calibration over Greater Paris, pp. 5085–5111.

Elessa Etuman, A., Coll, I., Makni, I., Benoussaid, T., 2020. Addressing the issue of exposure to primary pollution in urban areas: application to Greater Paris. Atmos. Environ. 239, 117661 https://doi.org/10.1016/j.atmosenv.2020.117661. ISSN 1352-2310. https://www.sciencedirect.com/science/article/pii/S1352231020303939.

European Environment Agency. Air Quality e-Reporting (AQ e-Reporting). www.eea.europa.eu/data-and-maps/data/aqereporting-2. Date last updated: October 30, 2017.

European Environment Agency, 2018. Air Quality in Europe — 2018 Report.

Fairburn, J., Schüle, S.A., Dreger, S., Karla Hilz, L., Bolte, G., 2019. Social inequalities in exposure to ambient air pollution: a systematic review in the WHO European region. Int. J. Environ. Res. Publ. Health 16 (17), 3127. https://doi.org/10.3390/ijerph16173127.

Guenther, A., Karl, T., Harley, P., Wiedinmyer, C., Palmer, P.I., Geron, C., 2006. Estimates of global terrestrial isoprene emissions using MEGAN (model of emissions of gases and aerosols from nature). Atmos. Chem. Phys. Discuss. 6, 107–173. https://doi.org/10.5194/acpd-6-107-2006.

Hatzopoulou, M., Miller, E.J., 2010. Linking an activity-based travel demand model with traffic emission and dispersion models: transport's contribution to air pollution in Toronto. Transport. Res. Transport Environ. 15, 315–325. https://doi.org/10.1016/j.trd.2010.03.007.

Hülsmann, F., Gerike, R., Ketzel, M., 2014. Modelling traffic and air pollution in an integrated approach - the case of Munich. Urban Clim. 10, 732–744. https://doi.org/10.1016/j.uclim.2014.01.001.

INSEE, 2015. Les zonages d'étude de l'Insee Une histoire des zonages supra communaux définis à des fins statistiques.

Janssens-Maenhout, G., Crippa, M., Guizzardi, D., Dentener, F., Muntean, M., Pouliot, G., Keating, T., Zhang, Q., Kurokawa, J., Wankmüller, R., Denier Van Der Gon, H., Kuenen, J.J.P., Klimont, Z., Frost, G., Darras, S., Koffi, B., Li, M., 2015. HTAP-v2.2: a mosaic of regional and global emission grid maps for 2008 and 2010 to study hemispheric transport of air pollution. Atmos. Chem. Phys. 15, 11411–11432. https://doi.org/10.5194/acp-15-11411-2015.

Kuenen, J.J.P., Visschedijk, A.J.H., Jozwicka, M., Denier Van Der Gon, H.A.C., 2014. TNO-MACC-II emission inventory; A multi-year (2003-2009) consistent high-resolution European emission inventory for air quality modelling. Atmos. Chem. Phys. 14, 10963–10976. https://doi.org/10.5194/acp-14-10963-2014.

McFadden, D., 1973. Conditional logit analysis of qualitative choice behavior. Front. Econom. https://doi.org/10.1108/eb028592.

Menut, L., Bessagnet, B., Khvorostyanov, D., Beekmann, M., Blond, N., Colette, A., Coll, I., Curci, G., Foret, G., Hodzic, A., Mailler, S., Meleux, F., Monge, J.-L., Pison, I., Siour, G., Turquety, S., Valari, M., Vautard, R., Vivanco, M.G., 2013. Chimere 2013: a model for regional atmospheric composition modelling. Geosci. Model Dev. (GMD) 6, 981–1028. https://doi.org/10.5194/gmd-6-981-2013.

Menut, L., Bessagnet, B., Siour, G., Mailler, S., Pennel, R., Cholakian, A., 2020. Impact of lockdown measures to combat Covid-19 on air quality over western Europe. Sci. Total Environ. 741, 140426 https://doi.org/10.1016/j.scitotenv.2020.140426. ISSN 0048-9697.

Monteiro, A., Durka, P., Flandorfer, C., Georgieva, E., Guerreiro, C., Kushta, J., Malherbe, L., Maiheu, B., Miranda, A.I., Santos, G., Stocker, J., Trimpeneers, E., Tognet, F., Stortini, M., Wesseling, J., Janssen, S., Thunis, P., 2018. Strengths and weaknesses of the FAIRMODE benchmarking methodology for the evaluation of air quality models. Air Qual Atmos Health 11, 373–383. https://doi.org/10.1007/s11869-018-0554-8.

Pascal, M., Corso, M., Chanel, O., et al., 2013. Assessing the public health impacts of urban air pollution in 25 European cities: results of the Aphekom project. Sci. Total Environ. 449, 390–400.

Skamarock, W.C., Klemp, J.B., Dudhi, J., Gill, D.O., Barker, D.M., Duda, M.G., Huang, X.-Y., Wang, W., Powers, J.G., 2008. A description of the advanced research WRF version 3. Tech. Rep. 113 https://doi.org/10.5065/D6DZ069T.

Solazzo, E., Bianconi, R., Pirovano, G., Matthias, V., Vautard, R., Moran, M.D., Wyat Appel, K., Bessagnet, B., Brandt, J., Christensen, J.H., Chemel, C., Coll, I., Ferreira, J., Forkel, R., Francis, X.V., 18 other authors, 2012. Operational model evaluation for particulate matter in Europe and North America in the context of AQMEII. Atmos. Environ. 53 (Special issue), 75–92.

STIF, 2012. Enquête globale transport: La mobilité en Île-de-France. Paris, France.

Theobald, M.R., Vivanco, M.G., Aas, W., Andersson, C., Ciarelli, G., Couvidat, F., Cuvelier, K., Manders, A., Mircea, M., Pay, M.-T., Tsyro, S., Adani, M., Bergstrom, R., Bessagnet, B., Briganti, G., Cappelletti, A., D'Isidoro, M., Fagerli, H., Mar, K., Otero, N., Raffort, V., Roustan, Y., Schaap, M., Wind, P., Colette, A., 2019. An evaluation of European nitrogen and sulfur wet deposition and their trends estimated by six chemistry transport models for the period 1990-2010. Atmos. Chem. Phys. 19, 379–405. https://doi.org/10.5194/acp-19-379-2019.

Thunis, P., Degraeuwe, B., Pisoni, E., Meleux, F., Clappier, A., 2017. Analyzing the efficiency of short-term air quality plans in European cities, using the CHIMERE air quality model. Air Quality, Atmosphere and Health 10 (2), 235–248. https://link.springer.com/article/10.1007/s11869-016-0427-y.

Timmermans, R.M.A., Denier van der Gon, H.A.C., Kuenen, J.J.P., Segers, A.J., Honoré, C., Perrussel, O., Builtjes, P.J.H., Schaap, M., 2013. Quantification of the urban air pollution increment and its dependency on the use of down-scaled and bottom-up city emission inventories. Urban Clim. 6, 44–62. https://doi.org/10.1016/j.uclim.2013.10.004.

World Health Organization, 2013. Review of Evidence on Health Aspects of Air Pollution – REVIHAAP Project. Technical Report. WHO Regional Office for Europe, Copenhagen. URL : http://www.ncbi.nlm.nih.gov/books/NBK361805/.

World Health Organization, 2016. Ambient Air Pollution: A Global Assessment of Exposure and Burden of Disease. World Health Organization.